Sodium-alginate-based proton-exchange membranes as electrolytes for DMFCs

S. Mohanapriya,[a] S. D. Bhat,[a] A. K. Sahu,[a] A. Manokaran,[a] R. Vijayakumar,[a] S. Pitchumani,[a] P. Sridhar[a] and A. K. Shukla*[b]

Received 16th April 2010, Accepted 2nd July 2010
DOI: 10.1039/c0ee00033g

Novel mixed-matrix membranes prepared by blending sodium alginate (NaAlg) with polyvinyl alcohol (PVA) and certain heteropolyacids (HPAs), such as phosphomolybdic acid (PMoA), phosphotungstic acid (PWA) and silicotungstic acid (SWA), followed by *ex-situ* cross-linking with glutaraldehyde (GA) to achieve the desired mechanical and chemical stability, are reported for use as electrolytes in direct methanol fuel cells (DMFCs). NaAlg-PVA-HPA mixed matrices possess a polymeric network with micro-domains that restrict methanol cross-over. The mixed-matrix membranes are characterised for their mechanical and thermal properties. Methanol cross-over rates across NaAlg-PVA and NaAlg-PVA-HPA mixed-matrix membranes are studied by measuring the mass balance of methanol using a density meter. The DMFC using NaAlg-PVA-SWA exhibits a peak power-density of 68 mW cm^{-2} at a load current-density of 225 mA cm^{-2}, while operating at 343 K. The rheological properties of NaAlg and NaAlg-PVA-SWA viscous solutions are studied and their behaviour validated by a non-Newtonian power-law.

Introduction

Direct methanol fuel cells (DMFCs) have advanced so much so that they are now classified as sixth fuel-cell-type.[1–3] However, DMFCs suffer from certain drawbacks, such as slow anode-kinetics and methanol crossover to the cathode.[4] The latter has a three-fold effect on DMFC systems: (i) decrease in the cell potential due to a mixed-potential reaction on the cathode, (ii) decrease in the overall fuel-utilization, and (iii) membrane degradation. To address the aforesaid problems, proton-conducting-methanol-impermeable membranes are being developed.[5–7]

In the literature, synthetic and natural polymers, like poly-(vinyl alcohol) PVA, chitosan (CS), and their composite membranes are reported to reduce the methanol cross-over in DMFCs.[8–10] However, these membranes suffer from excessive swelling in aqueous media. By contrast, cross-linked polystyrene sulfonic acid-co-maleic anhydride (PSSA-MA) semi-inter-penetrating membranes exhibit controlled-charge-density that prevents their swelling in aqueous medium with proton conductivity values of $\sim 10^{-2}$ S cm^{-1} under fully-humidified conditions.[11] Our earlier findings suggest that PVA-PSSA blend and mordenite-PVA-PSSA composite membranes help mitigating methanol cross-over in DMFCs.[12,13] It is also demonstrated that cost-effective natural polymeric membranes based on CS and hydroxyethylcellulose (HEC) mixed-matrix membrane can be effectively used in DMFCs.[14]

Biopolymers are both eco-friendly and cost effective, and among these, sodium alginate (NaAlg), derived from marine algae, is a non-toxic anionic bio-copolymer comprising β-D-mannuronate (M) and α-L-guluronate (G) in varying ratios.[15,16] NaAlg is one of the polysaccharides that can act as a membrane material with preferential water sorption during pervaporative separation of azeotropic mixtures.[17,18] However, the pristine NaAlg membrane suffers from excessive swelling and has poor mechanical stability. Accordingly, in the present study, NaAlg is blended with semi-crystalline, bio-compatible synthetic polymer PVA that possesses good hydrophilicity, flexibility and mechanical strength.[19] This also leads to good compatibility, unique physico-chemical, mechanical and morphological properties leading to the formation of a polymeric network with a micro-domain structure.[20,21] However, NaAlg-PVA blend

[a]*CSIR-Central Electrochemical Research Institute-Madras Unit, Chennai, 600113, India*
[b]*Solid State and Structural Chemistry Unit, Indian Institute of Science, Bangalore, 560012, India. E-mail: shukla@sscu.iisc.ernet.in; Fax: +91-80-23601310; Tel: +91- 80-23603282*

Broader context

Natural polysaccharides as biopolymers are environmentally benign and hence are widely used in developing membranes for a variety of applications. Among the various natural polymers, sodium alginate (NaAlg) is a water-soluble polysaccharide with good membrane forming properties. The present study is an attempt to fine tune and custom design NaAlg-based membrane electrolytes for use in direct methanol fuel cells (DMFCs). A new polymer electrolyte membrane, reported in this study by blending natural-polymer NaAlg and synthetic-polymer polyvinyl alcohol (PVA), exhibits appreciable proton-conductivity on incorporating heteropolyacids and restricts methanol crossover in DMFCs.

 This journal is © The Royal Society of Chemistry 2010

exhibits poor proton-conductivity and hence an effort has been made to improve the proton conductivity of the blend by incorporating heteropoly acids (HPAs).

HPAs are known to have transition-metal and oxygen-anion clusters with varying molecular size, composition and architecture.[22] The molecular Keggin-anion structure of HPA comprises a central tetrahedron (XO_4^{n-}) surrounded by 12 linked octahedral units ($M_{12}O_{36}$) containing the addenda atom (M).[23] The delocalized charge on the central tetrahedron stabilizes the Keggin anion.[24] Nakemura *et al.*[25] are the first to explore the use of HPAs in fuel-cell application that has invoked interest in HPA-based composite membranes for such applications.[26–31] However, high water-solubility of HPA causes performance degradation in fuel cells as the product water leaches out HPA.[32] Therefore, efforts are being spent to stabilise HPA by partially exchanging its protons with larger Cs cations[33] in order to arrest HPA leach-out from the mixed matrices. The insolubility of Cs-salt of HPA arises due to the higher lattice energy associated with Cs salt compared to pristine HPA. Cs salt stabilised HPA has a surface area > 100 $m^2\ g^{-1}$, a value higher than pristine HPA.[34]

The present study is an attempt to explore the effect of Cs-stabilized HPAs, namely, PMoA, PWA and SWA in NaAlg-PVA blend, for achieving good proton conductivity with reduced methanol permeability and to enhance the electrochemical selectivity. The DMFC comprising NaAlg-PVA-SWA mixed matrix-membrane exhibits a peak power-density of 68 mW cm^{-2} at a load current-density of 225 mA cm^{-2} while operating at 343 K with oxidant feed at atmospheric pressure.

Experimental

Materials

Sodium alginate (NaAlg) and poly(vinyl alcohol) (PVA), (99.7% hydrolyzed, M.W. 115,000) were obtained from Loba Chemie, India. Phosphotungstic acid (PWA), phosphomolybdic acid (PMoA) and caesium carbonate were procured from Acros organics. Silicotungstic acid (SWA) was obtained from SRL chemicals. Glutaraldehyde (25% aqueous) and sulfuric acid (98%) were obtained from S.D. Fine Chemicals, India. All chemicals were used as-received. Toray TGP-H-120 was procured from *E*-Tek (US). Vulcan XC-72R carbon was procured from Cabot Corporation (US). Pt–Ru (60 wt% in 1 : 1 atomic ratio) and Pt/C (40 wt% Pt on Vulcan XC-72R carbon) were obtained from Alfa Aesar (Johnson Matthey). Deionised (DI) water (18.4 MΩ cm) from Millipore was used during the experiments.

Stabilization of HPAs

HPAs were stabilized with caesium carbonate similar to the procedure described elsewhere.[35,36] In brief, stoichiometric amounts of caesium carbonate in deionised water were added to the transparent, homogenous aqueous HPA solution which turned cloudy and precipitated out ion-exchanging the protons with caesium carbonate solution. The resulting admixture was sonicated in an ultrasonic bath for 4 h and allowed to dry in an air-oven at 303 K. The HPAs thus obtained were heat-treated for 3 h at 573 K and ground to fine powder. Attempts were made to control the number of protons substituted by controlling the stoichiometry of the added salt solution, namely Cs:HPAs in 1 : 0.5 molar ratio, enabling one H^+-ion from HPA to exchange with caesium to stabilize it in aqueous/acidic medium.

Membrane preparation

NaAlg-PVA-HPA mixed-matrix membranes were prepared by a solution-casting technique. In brief, 30 mL of 4 wt% PVA solution was prepared by dissolving the required amount of PVA in water at 333 K followed by its mechanical stirring until a clear solution was obtained. Similarly, 20 mL of 25 wt% NaAlg in relation to PVA was dissolved in aqueous medium at 303 K followed by its stirring until a homogeneous solution was obtained. Both solutions were mixed and further stirred for 4 h to form a compatible blend. Similarly, varying compositions of stabilized HPAs, namely, PMoA, PWA and SWA were dispersed separately in water under ultrasonication for 2 h and added to NaAlg-PVA solution under continuous stirring for 3 h. The composition of HPAs was varied between 10 and 90 wt% in the polymer matrix prior to its optimization at 40 wt% of HPA with respect to NaAlg-PVA matrix forming mixed matrices. The viscous solution was cast on a flat Plexiglass plate to form a membrane by evaporating the solvent at room temperature (~303 K). NaAlg-PVA blend membrane was prepared in a similar manner without the addition of HPAs. The membranes were peeled off from the plate after drying and *ex-situ* cross-linked in a solution containing isopropanol (IPA)-water mixture in 9 : 1 ratio, and mol% of glutaraldehyde (GA) was varied between 0.5 and 2 mol% to achieve different cross-linking densities; 1 vol.% HCl was used to catalyse the cross-linking reaction. After cross-linking, the membranes were copiously washed in deionised water to remove traces of unreacted glutaraldehyde and residual HCl. The membranes were dried at room temperature and the thickness of the membranes was ~ 170 μm. It is noteworthy that, in relation to the polymeric matrix, the membrane was more brittle with HPA content > 40 wt%.

Additive stability in the mixed-matrix membranes

The solubility and stability of caesium-stabilized HPAs in NaAlg-PVA matrix were evaluated following the procedure reported elsewhere.[34] In brief, the stability of HPA in aqueous media at 343 K was determined by heating pieces of the mixed matrices in an oven at 342 K for 1 h and immersing pieces of known weight into hot H_2SO_4 (1M at 358 K) for 2 h followed by washing in hot de-ionised water (358 K). The membrane pieces were dried in an oven at 342 K for 1 h followed by weighing. Similarly, the additive stability of pristine HPAs was also determined. The difference in weight was taken as the loss of additive.

Ion-exchange capacity

The ion-exchange capacity (IEC) indicates the number of milli-equivalents of ions in 1 g of the mixed-matrix membrane. To estimate IEC, membranes of similar weights were soaked in 50 mL of 0.01 N sodium hydroxide solutions for 12 h at room temperature (303 K) and 10 mL of the solution was titrated against 0.01 N sulfuric acid.[13] The sample was regenerated with

1 N hydrochloric acid, washed copiously with water to remove acid and dried to a constant weight. IEC was estimated from eqn (1) given below.

$$\mathrm{IEC} = \frac{(B-P)\mathrm{x}0.01\mathrm{x}5}{m} \quad (1)$$

In eqn (1), IEC = ion exchange capacity (in meq g^{-1}), B = amount of sulfuric acid used to neutralize blank sample solution in mL, P = amount of H_2SO_4 used to neutralize the mixed-matrix membrane soaked solution in mL, 0.01 = normality of H_2SO_4, 5 = the factor corresponding to the ratio of the amount of NaOH used to soak the mixed-matrix membrane to the amount used for titration, and m = membrane mass in g.

Sorption and proton-conductivity measurements

For sorption measurements, circularly cut (diameter = 2.5 cm) Nafion-117, NaAlg-PVA blend and NaAlg-PVA-HPA mixed-matrix membranes were dipped in de-ionised water for 24 h to attain equilibrium. The membranes were surface blotted and initial mass values were recorded on a single-pan digital micro-balance (Sartorius, Germany) within an accuracy of ±0.01 mg. The membranes were then dried in a vacuum oven at 373 K for 24 h and their respective weights were measured. Sorption values for the aforesaid membranes were calculated using eqn (1) given below.

$$\%\mathrm{Sorption} = \left(\frac{W_\infty - W_\circ}{W_\circ}\right)\times 100 \quad (2)$$

In eqn (2), W_∞ and W_o refer to the weights of sorbed and dry membranes, respectively.

Proton conductivity measurements were performed on Nafion-117, NaAlg-PVA blend and NaAlg-PVA-HPA mixed-matrix membranes in a two-probe cell by the AC impedance technique. The conductivity cell comprised two stainless-steel electrodes, each of 20 mm in diameter. The membrane sample was sandwiched between these two electrodes mounted in a Teflon block and kept in a closed glass-container. The ionic conductivity data for the membranes were obtained under fully-humidified conditions (100%) by keeping deionized water at the bottom of the test container and equilibrating it for ~24 h. Subsequently, conductivity measurements were conducted between 303 and 373 K in a glass container with the provision to heat. The temperature was constantly monitored with a thermometer kept inside the container adjacent to the membrane. AC impedance spectra of the membranes were recorded in the frequency range between 1 MHz and 10 Hz with 10 mV amplitude using an Autolab PGSTAT 30. The resistance (R) of the membrane was determined from the high-frequency intercept of the impedance with the real axis and the membrane conductivity was calculated from the membrane resistance, R, from:

$$\sigma = \frac{l}{RA} \quad (3)$$

In eqn (3), σ is the proton conductivity of the membrane in S cm^{-1}, l is the membrane thickness in centimetres and A is the membrane cross-sectional area in cm^2.

Physicochemical characterization

Universal testing machine (UTM) (Model AGS-J, Shimadzu) with an operating head-load of 10 kN was used to study the mechanical properties of the membranes. The cross-sectional area of the sample was obtained from the initial width and thickness of the membrane sample. The test samples were prepared in the form of a dumb-bell shaped object as per ASTM D-882 standards. The membranes were then placed in the sample holder of the machine. The film was stretched at a cross-head speed of 1 mm min^{-1} and its tensile strength was estimated using eqn (4).

$$\text{Tensile strength (N mm}^{-2}) = \frac{\text{Maximum load}}{\text{Cross sectional area}} \quad (4)$$

Surface micrographs for NaAlg-PVA blend membrane and HPA-NaAlg-PVA mixed-matrix membranes were obtained using JEOL JSM 35CF Scanning Electron Microscope (SEM). Gold film of thickness < 100 nm was sputtered on the membrane surfaces using a JEOL Fine Coat Ion Sputter-JFC-1100 Unit, prior to their examination under SEM. Thermogravimetric analyses of all the membranes were carried out using a SDT Q600 V8.2 TGA/DTA instrument in the temperature range between 273 and 1073 K at a heating rate of 5 K min^{-1} with nitrogen flushed at 200 mL min^{-1}. The FTIR spectra for NaAlg-PVA blend and NaAlg-PVA-SWA mixed-matrix membranes were obtained using a Nicolet IR 860 spectrometer (Thermo Nicolet Nexus-670) in the frequency range between 4000 and 400 cm^{-1}.

Rheological measurements

The rheological properties of NaAlg and NaAlg-PVA-SWA viscous solutions were measured in a dynamic flow mode isothermally at 303 K using Physica MCR 51 rheometer (Antonpar, Germany). Experiments at an imposed shear rate were performed on DG26 (Double Gap), fitted with parallel plate geometry. The quantity of the fluid on the plate was 4 mL and temperature was controlled by Viscotherm VT2 system. The relative viscosities of the above solutions were determined in relation to the shear rate.

Membrane-performance evaluation in DMFC

The performances of all the membranes were evaluated in a DMFC by making membrane electrode assemblies (MEAs). In brief, both the anode and cathode comprised a backing layer, a gas-diffusion layer (GDL) and a reaction layer. Teflonised Toray carbon papers (thickness = 0.38 mm) were employed as the backing layers for these electrodes. A diffusion layer comprising 1.5 mg cm^{-2} of Vulcan XC-72R carbon slurry dispersed in cyclohexane was applied onto the backing layers followed by sintering in a muffle furnace at 623 K for 30 min. 60 wt% Pt–Ru (1 : 1 atomic ratio) supported on Vulcan XC-72R carbon mixed with binder and coated on to one of the GDLs constituted the catalyst layer on the anode while 40 wt% Pt catalyst supported on Vulcan XC-72R carbon mixed with binder coated onto the other GDL constituted the catalyst layer on the cathode. The catalyst loading on both the anode and cathode was kept at 2 mg cm^{-2}. The active area for the DMFC was 4 cm^2. MEAs comprising NaAlg-PVA blend and NaAlg-PVA-HPA

This journal is © The Royal Society of Chemistry 2010

mixed-matrix membranes were obtained by hot pressing at 15 kN ($\sim$ 60 kg cm^{-2}) at 353 K for 2 min. MEAs were evaluated using a conventional fuel-cell fixture with a parallel serpentine flow-field machined on graphite plates. The cells were tested at 343 K with 2 M aqueous methanol at a flow rate of 2 mL min^{-1} at the anode side and oxygen at the cathode side at a flow rate of 300 mL min^{-1} at atmospheric pressure. The cell voltage and power density in relation to the current density were measured galvanostatically using an Arbin Fuel Cell Test Station (Model PEM-FCTS-158541).

Methanol-permeation studies

In the literature, it is reported that methanol crossover can be measured by measuring the CO_2 concentration of cathode exhaust gases which is measured by (a) mass spectroscopy, (b) gas chromatography, (c) gas analyzer and (d) CO_2 gas sensor. These measurements do not account for CO_2 permeation across the membrane and hence could be erroneous. The density measurement is free from the above problem. Determination of methanol crossover using density measurement method has already been reported in the literature.[37,38]

The permeated methanol from anode to cathode was measured by determining the methanol concentration based on the mass balance between the methanol supplied into the cell, methanol utilized for the electrochemical reaction and unutilized methanol during the DMFC operation. The approach follows the Faraday concept,[39] where the concentration of methanol varies with the load current-density with one mole of methanol being equivalent to 96485 C. Accordingly, the amount of the methanol crossed-over ($MeOH_{cross\text{-}over}$) was taken as the difference between the amounts of methanol circulated inside the cell ($MeOH_{cir}$) for the reaction and the methanol consumed during the faradaic reaction to produce electrical energy ($MeOH_{rxn}$).

2 M aqueous methanol was initially supplied into the DMFC and the cell was allowed to equilibrate. After reaching a steady state, the difference in the amount of methanol supplied to the cell and the methanol collected in the anode outlet for a particular time period (t) was measured under OCV conditions and also at varying load current-densities at 343 K under ambient pressure. The densities of methanol collected from the inlet and outlet of the cell anode were measured using a density meter (Mettler Toledo, DB51) by taking 20 mL of the collected methanol sample. Subsequent to each measurement, the density meter was purged with water and IPA followed by aqueous methanol solution. The molarity of the methanol was calculated from the measured density values using eqn (5) given below.[40]

$$\text{Molarity} = 10 \text{ wt\% of methanol} \left(\frac{\rho}{M}\right) \quad (5)$$

In eqn (5), ρ is the density of methanol (g cm^{-3}) and M is the molecular weight of methanol (g mol^{-1}).

Inlet methanol concentration (C_1) and volume (V_1) of methanol and the outlet methanol concentration (C_2) and volume (V_2) were measured separately after the cell operation had stopped. It is noteworthy that under OCV conditions, methanol supplied at the inlet ($MeOH_{in}$) is equal to the sum of the methanol collected at the outlet ($MeOH_{out}$) and that crossed over ($MeOH_{cross\text{-}over}$) from the anode to the cathode side of the cell. Accordingly,

$$MeOH_{cross\text{-}over} = MeOH_{in} - MeOH_{out} \quad (6)$$

At a particular current density (I), the methanol consumed during the electrochemical oxidation reaction for a time period (t) was calculated from eqn (7) given below.

$$MeOH_{rxn} = I \times 4.19 \times 10^{-3} \times t \quad (7)$$

In eqn (7), I is in A, t is in min and 4.19×10^{-3} ml A^{-1} min^{-1}). Methanol cross-over was calculated from eqn (6) and (7) at varying currents.

Accordingly,

$$MeOH_{\text{ cross-over }} = MeOH_{cir\text{-}in/out} - MeOH_{rxn} \quad (8)$$

$MeOH_{cir\text{-}in/out}$ is the difference in methanol volume at the inlet and outlet of the anode. From eqn (8), the equivalent current ($i_{pmtMeOH}$, mA cm^{-2}) for methanol cross-over from anode to cathode side was determined.[41]

Results and discussion

Cross-linking density of membranes

Fig. 1 shows the % sorption and tensile strength in relation to cross-linking density of NaAlg-PVA membranes. The water uptake decreases with the increase in cross-linking density of the membrane from 0.5 to 2 mol% as the increased cross-linked networks formed at higher cross-link density restrict the swelling of the blend membranes.[42] It is noteworthy that tensile strength increases with cross-linking density thereby exhibiting increased membrane rigidity.

Ion-exchange capacity (IEC) of membranes

IEC is an indication of the content of ionic groups present in a polymeric matrix responsible for the proton conduction and thus provides an indirect approximation of the proton conductivity. For Nafion-117, IEC value is 0.9 meq/g,[43] while the measured IEC value for NaAlg-PVA blend membrane is 0.678 meq g^{-1}. For the mixed matrices, namely NaAlg-PVA-PWA, NaAlg-PVA-PMoA and NaAlg-PVA-SWA, measured

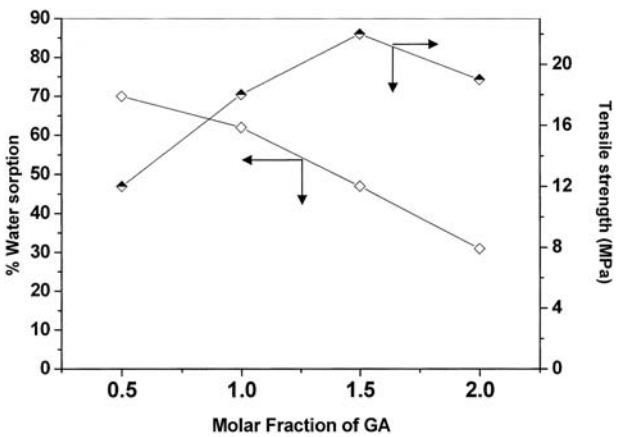

Fig. 1 Water sorption (%) and tensile strength *vs.* molar fraction of GA for NaAlg-PVA blend.

IEC values are 0.85, 0.841 and 0.873 meq g^{-1}, respectively, which suggest an increased mobility of exchanged ions in hydrated HPAs. It is noteworthy that a marginal difference in the IEC values of mixed matrices is observed, indicating that the conductivity values for different HPAs do not vary drastically.

Sorption and additive stability of membranes

Liquid sorption through polymeric membranes has been well documented in the literature.[44] Sorption data for Nafion-117 membrane, NaAlg-PVA blend and NaAlg-PVA-HPA mixed matrices at 343 K in water are presented in Fig. 2. It is noteworthy that sorption for NaAlg-PVA blend increases after addition of HPAs. This is attributed to the degree of hydration varying from 30 to 6 molecules of water hydration per HPA molecule,[36] wherein HPAs usually exist in hydrated phases and increase the degree of swelling for the mixed matrices. However, for Nafion-117 membrane, water sorption is lower due to the presence of both hydrophilic pendent chains and hydrophobic fluorinated backbone.[7] By contrast, due to the dual hydrophilic interactions between the NaAlg-PVA blend and HPAs, the water sorption increases and becomes predominant for NaAlg-PVA-SWA mixed matrix-membrane. Similarly, the additive stability for HPAs is quantified by the weight-loss measurements which show negligible weight loss for stabilized HPAs in the mixed-matrix membrane in relation to the weight loss observed for pristine HPAs in the mixed matrices. This suggests that an unsubstituted portion of the HPA leaches out, leaving behind the partially substituted HPAs in the mixed matrices.

Proton conductivity of membranes

Proton transport occurs by the Grötthus and vehicular mechanisms where the protons jump from one solvent molecule to the other through hydrogen bonds, or diffuse together with solvent molecules, respectively.[45] Higher water uptake promotes proton transport while higher IEC decreases the distance between anionic groups leading to faster proton conduction.[11] At room temperature, high water sorption and IEC help protons transport faster than the diffusion of water, suggesting involvement of intermolecular proton transfer during the mobility of protons, a process termed as structural diffusion.[46] The presumptive

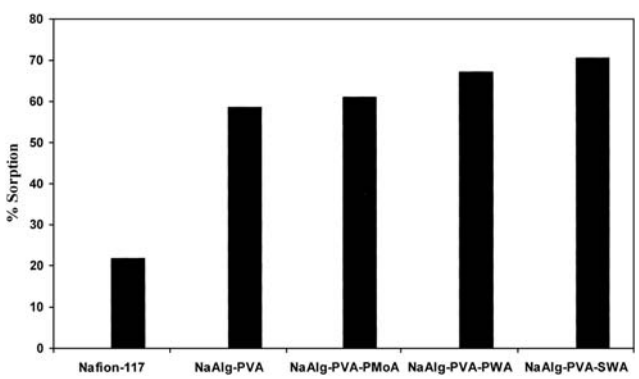

Fig. 2 % water sorption for Nafion-117, NaAlg-PVA blend, NaAlg-PVA-PWA, NaAlg-PVA-SWA and NaAlg-PVA-PMoA mixed-matrix membranes.

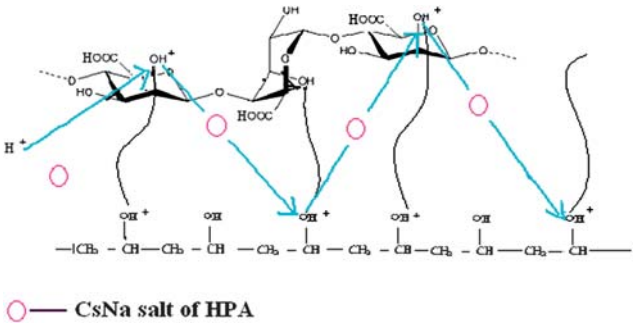

Scheme 1 Presumptive view of proton transfer involving Grötthus (hopping) mechanism in NaAlg-PVA-HPA mixed-matrix membrane.

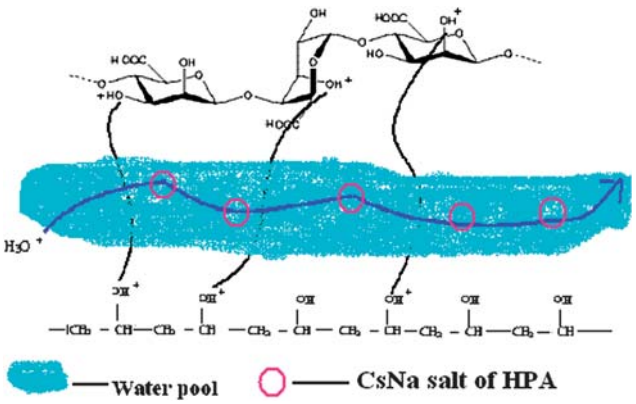

Scheme 2 Presumptive view of proton transfer involving vehicular mechanism in NaAlg-PVA-HPA mixed-matrix membrane.

proton conduction Grötthus mechanism through NaAlg-PVA-HPA mixed-matrix membrane is shown in Scheme 1. In all the HPA-NaAlg-PVA mixed-matrix membranes, molecular diffusion dominates intermolecular proton transfer with increasing temperature.[47] The presumptive proton conduction vehicular mechanism in NaAlg-PVA-HPA mixed-matrix membrane is shown in Scheme 2.

The proton conductivity of NaAlg-PVA-HPA mixed-matrix membranes is higher than the NaAlg-PVA blend-membrane. The distinct hydrophilicity of HPAs is beneficial in enhancing the proton conduction by forming hydrogen bonds between NaAlg-PVA blend and $[XM_{12}O_{40}]^{n-}$ anion. Sorption characteristics have a profound influence on membrane conductivity as higher water sorption facilitates proton transport through the membrane, leading to faster proton conduction. It is noteworthy that NaAlg-PVA-SWA mixed-matrix membrane exhibits higher proton conductivity than NaAlg-PVA-PWA and NaAlg-PVA-PMoA mixed-matrix membranes. The differences in ionic conductivity can be explained on the basis of the chemical compositions of HPAs. Although all HPAs studied here have a Keggin type of anion in their structure, the atom present in the central tetrahedron is silicon for SWA, while it is phosphorus for PWA and PMoA. Owing to the lower valency and electronegativity of silicon, SWA anion has a charge of 4^-, whereas it is 3^- both for PWA and PMoA anions. An additional proton present in SWA is responsible for increased ionic conductivity that takes full advantage of NaAlg-PVA polymeric voids.[48] The

This journal is © The Royal Society of Chemistry 2010

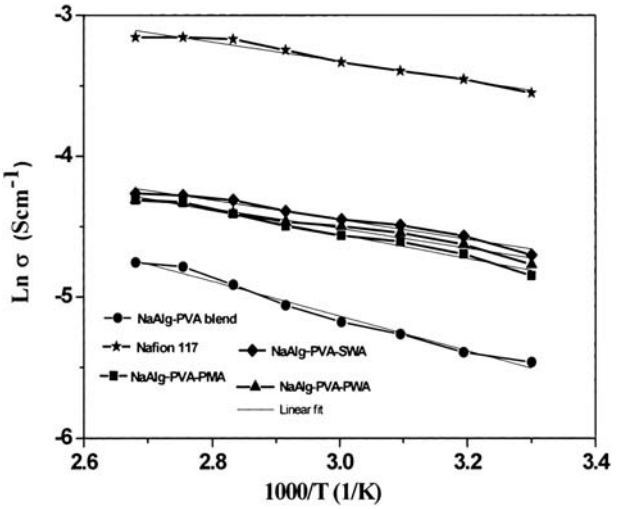

Fig. 3 ln σ *vs.* 1000/T plot for Nafion-117, NaAlg-PVA blend, NaAlg-PVA-PWA, NaAlg-PVA-SWA and NaAlg-PVA-PMoA mixed-matrix membranes.

lower ionic conductivity of PMoA in relation to PWA is attributed to the increased stability of Keggin anion in PWA that enhances the acid strength of PWA.[49]

All membranes exhibit an Arrhenius-type temperature dependence of proton conductivity suggesting a thermally-activated process. The activation energy, which is the minimum energy required for proton transport, is obtained from the slope of the Arrhenius plots obtained by plotting ln σ *vs.* 1/T according to eqn (9) given below.

$$\sigma = \sigma_o e^{-(E_a/RT)} \quad (9)$$

In eqn (9), σ is the proton conductivity in S cm^{-1}, σ_0 is the pre-exponential factor, E_a is the activation energy in kJ mol^{-1}, R is the universal gas constant (8.314 J mol^{-1} K), and T is the absolute T/K.

Since the proton-conduction process is thermally activated, conductivity increases with increasing temperature as shown in Fig. 3. From the data, E_a value for NaAlg-PVA blend membrane is found to be 29.2 kJ mol^{-1} while the E_a values for NaAlg-PVA-PWA, NaAlg-PVA-SWA and NaAlg-PVA-PMoA mixed matrices are found to be 23.5, 20.4 and 24.9 kJ mol^{-1}, respectively. These data suggest that E_a for proton conduction decreases with the incorporation of HPA in the NaAlg-PVA matrix. The lower activation energy observed for the NaAlg-PVA-HPA mixed-matrix membranes in relation to NaAlg-PVA blend membrane facilitates more protons to transfer through the mixed-matrix membrane; E_a value of 16.02 kJ mol^{-1} observed for Nafion-117 membrane suggests that the activation energy is much lower than the other membranes facilitating higher proton conductivity in the former.

Mechanical stability of membranes

The mechanical properties of all the membranes were determined by its tensile strength and the percentage elongation-at-break, and the data are presented in Table 1. The data suggest that the tensile strength for the NaAlg-PVA blend membranes increases

Table 1 Properties of Nafion-117, NaAlg-PVA blend and NaAlg-PVA-HPA mixed- matrix membranes

Membrane type	Tensile strength/ 10^6 N m^{-2}	Elongation-at-break (%)	Arrhenius activation energy/kJ mol^{-1}	Electrochemical selectivity/ 10^{10} S s m^{-3}
NaAlg-PVA	21.5	34	29.2	2.12
NaAlg-PVA -PWA	34.8	25	23.5	3.89
NaAlg-PVA -PMoA	35.2	22	24.9	3.69
NaAlg-PVA -SWA	38.6	24	20.4	4.19
Nafion 117	78.5	125	16.1	7.06

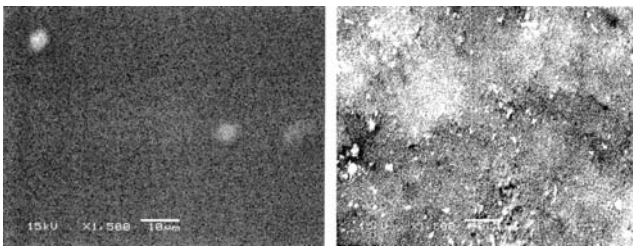

Fig. 4 Scanning electron micrographs for (a) NaAlg-PVA blend and (b) NaAlg-PVA-SWA mixed-matrix membranes.

when HPA is incorporated into the matrix. Introduction of HPAs in to NaAlg-PVA polymeric matrix restricts the chain segmental mobility and increases the membrane strength. By contrast, elongation-at-break for NaAlg-PVA-HPA mixed-matrix membrane decreases due to the increased membrane rigidity. Interaction of HPA with the NaAlg-PVA polymeric chains is further validated by these data. However, the tensile strength and percentage elongation of these membranes in hydrated conditions is lower than Nafion-117.[43]

Morphological evaluation of membranes

SEM pictures showing the surface morphology of NaAlg-PVA blend and HPA-NaAlg-PVA mixed-matrix membranes are presented in Fig. 4 (a) and (b). The smooth surface morphology shown in Fig. 4(a) reveals the homogeneity and good compatibility of NaAlg-PVA polymeric matrix. The typical surface morphology of NaAlg-PVA-SWA mixed-matrix membrane shown in Fig. 4 (b) is comparatively rougher, suggesting the distribution of SWA particles as a dispersed phase in the NaAlg-PVA matrix.

Thermogravimetric analysis of membranes and HPAs

TGA data for pristine NaAlg-PVA blend and NaAlg-PVA-HPA mixed-matrix membranes and pristine HPAs are shown in Fig. 5. The 3 main degradation stages occur due to the processes of thermal solvation, thermal degradation and thermal oxidation of the polymeric matrices as reported for similar kind of membranes.[14] As shown in the inset to Fig. 5, PWA displayed only one-step weight loss (~1%) upon heating from room temperature to about 373 K due to the evaporation of absorbed moisture, but no significant weight loss above 373 K is observed

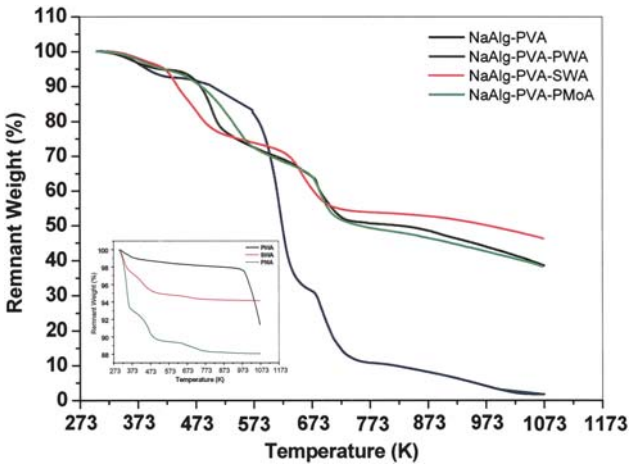

Fig. 5 TGA plots for (a) NaAlg-PVA blend (b) NaAlg-PVA-PWA (c) NaAlg-PVA-SWA (d) NaAlg-PVA-PMoA mixed-matrix membranes. Inset shows TGA plots for pristine HPAs.

indicating the absence of crystalline water.[50] Unlike PWA, SWA and PMoA exhibit a two-stage and three-stage weight loss stages, respectively. The second-stage weight loss (~3%) observed for SWA and PMoA between ~373 and ~523 K is most likely due to the evaporation of crystalline water. For PMoA, the third-stage weight loss (1%) between ~523 and ~773 K is attributed to the evaporation of more tightly bonded water.[51] By comparing the starting temperatures of the second-stage weight loss, the thermal stability varies as: NaAlg-PVA > NaAlg-PVA-PWA ≈ NaAlg-PVA-PMoA > NaAlg-PVA-SWA. Moreover, the weight loss at this stage is mainly due to the decomposition of the polymers (NaAlg-PVA) as the weight loss due to the evaporation of crystalline water is rather low. Accordingly, the introduction of HPAs to the NaAlg-PVA membranes will induce membrane rigidity, affecting the thermal stability. This, however, would not be a constraint as the operating temperature of DMFCs was kept below 100 °C. By contrast, first weight-loss between 273 and 423 K is due to loss of absorbed water. The second weight-loss between 423 and 673 K is due to cleavage of NaAlg-PVA chains and removal of crystalline water from HPA present in the mixed matrices. A major weight loss of 30% for SWA-based mixed-matrix membranes and 40% for PWA and PMoA-based mixed-matrix membranes is observed at the second stage. Decomposition of the main polymer chains and acetal linkage created during the cross-linking also contributes to second weight loss.[52] Third weight-loss between 673 and 1073 K for all the mixed matrices is due to thermal degradation of cleaved polymeric chains accompanied by structure collapse of the HPAs.[53]

Fourier-transform infrared (FTIR) spectroscopy

Typical FTIR spectra of NaAlg-PVA blend and NaAlg-PVA-SWA mixed-matrix membranes are shown in Fig. 6. A broad band centred at ~3500 cm^{-1} relates to intermolecular hydrogen bonding and –OH stretching vibration of PVA. The characteristic peak ~1032 cm^{-1} is due to the stretching vibration attributed to the cross-linking reaction of the hydroxyl groups of NaAlg and PVA with the aldehyde groups of glutaraldehyde. The peaks

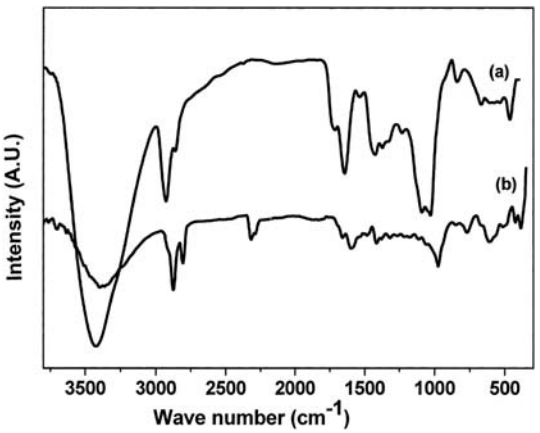

Fig. 6 FTIR spectra for (a) NaAlg-PVA blend (b) NaAlg-PVA-SWA mixed-matrix membranes.

at 1310 cm^{-1}, 1125 cm^{-1} and 1094 cm^{-1} are attributed to C–C–H and O–C–H deformation, C–O stretching and C–O and C–C stretching vibrations of pyranose rings present in NaAlg.[54] Four kinds of oxygen atoms present in the Keggin unit of SWA are the central oxygen atoms (O_a), corner-sharing bridging oxygen atoms (O_b), edge-sharing bridging oxygen atoms (O_c) and terminal oxygen atoms (O_d).[39] The characteristic peaks of Keggin anion at ~985, ~890 and ~800 cm^{-1} appear as shoulders and merge, forming a broad band at 899 cm^{-1}. The distinct peak due to $W = O_t$ band at around 980 cm^{-1} is suppressed indicating the protons in SWA to be partially substituted by Cs atoms.[36] The peaks observed at 1064 and 1237 cm^{-1} are due to the asymmetric stretching vibrations of the central PO_4 tetrahedron of Keggins structure.[14] The positions of the vibration modes of all types of metal-oxygen (W–O) bonds are strongly influenced by an interaction of heteropolyacid with the polymer. The stretching of W–O–W bond with corner sharing oxygen (O_c) of SWA in the NaAlg-PVA is red-shifted from 878 to 825 cm^{-1} due to the coulumbic interaction between the hydroxyl groups of the NaAlg-PVA and SWA.

Rheological behaviour of polymer solutions

The rheological behaviour of typical NaAlg and NaAlg-PVA-SWA viscous polymer solutions is classically evaluated by the variation of viscosity (μ) in relation to the shear rate ($\delta u/\delta y$). From Fig. 7(a), it is evident that the viscosity of polymer solutions varies non-linearly with increase in shear rate. Viscosity is higher at lower shear rate and *vice versa* exhibiting a typical shear-thinning behaviour owing to the decrease in viscosities of NaAlg and NaAlg-PVA-SWA with increase in shear rate. Materials possessing shear-thinning behaviour are termed pseudoplastics.[55] In the present study, NaAlg and NaAlg-PVA-SWA have lower viscosities at higher shear rates representing pseudoplastic behaviour of the polymer solutions.

Both NaAlg and NaAlg-PVA-SWA viscous solutions follow a similar trend in their flow characteristics under the adapted experimental conditions as shown in Fig. 7(a) and 7(b). However, the relative viscosity of NaAlg changes after the introduction of SWA, indicating the existence of some intramolecular interaction between the polymeric chains. SWA incorporation to the

 This journal is © The Royal Society of Chemistry 2010

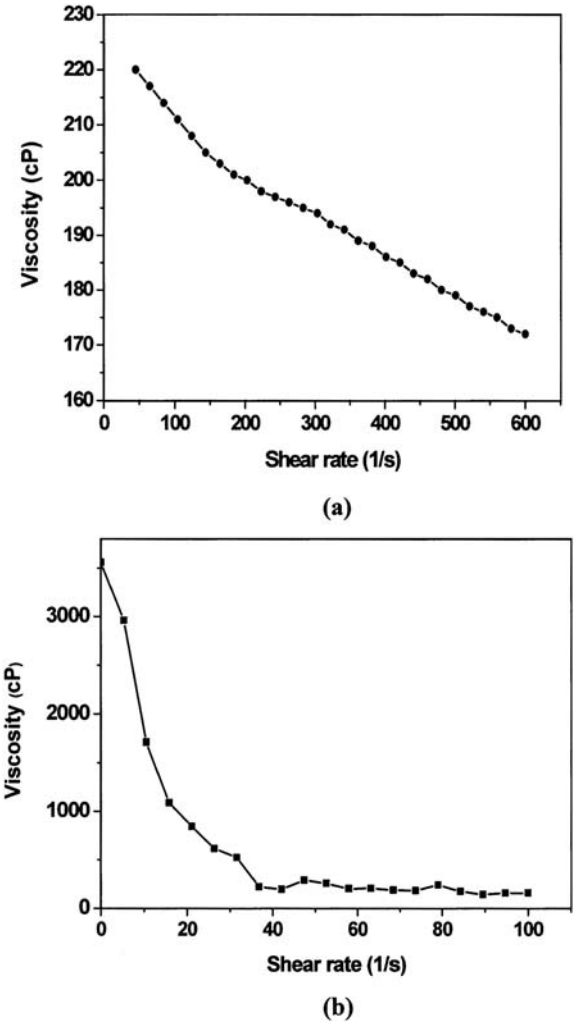

Fig. 7 Viscosity *vs.* shear rate plots for (a) NaAlg (b) NaAlg-PVA-SWA viscous solutions.

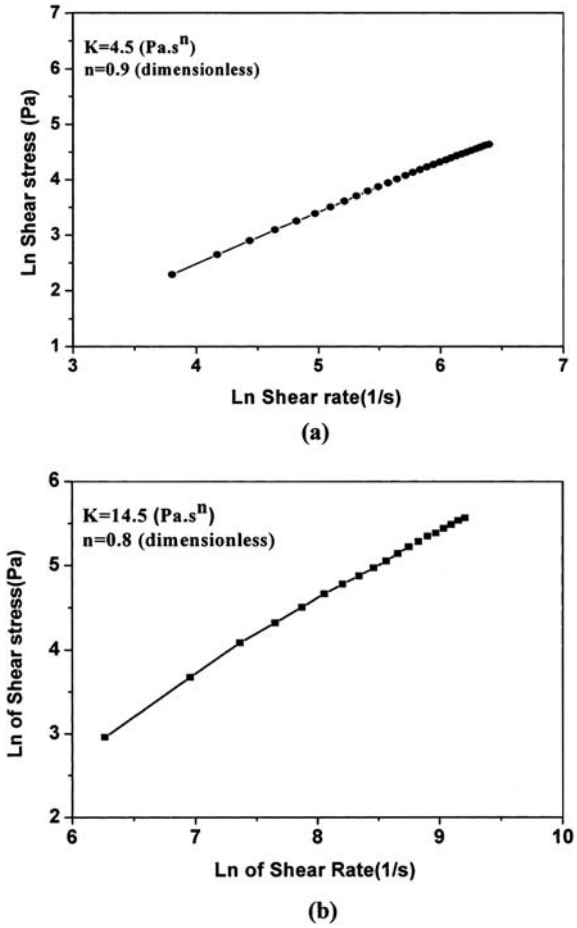

Fig. 8 Power law plots for (a) NaAlg (b) NaAlg-PVA-SWA viscous solutions. Inset shows the power law parameters.

NaAlg-PVA blend restricts the flow velocity that increases viscosity. SWA particles interact with the NaAlg-PVA chains, affecting the segmental mobility of the polymeric matrix.

The typical flow behaviour of NaAlg and NaAlg-PVA-SWA viscous solutions is described by the Non-Newtonian power law[56] given by eqn (10).

$$\mu = K(\delta u/\delta y)^{n} \tag{10}$$

In eqn (10), K is the flow consistency index (Pa s^{n}), $\delta u/\delta y$ is the shear rate or velocity gradient (1/s), and n is the flow behaviour index.

The power-law plots for NaAlg and NaAlg-PVA-SWA are shown in Fig. 8(a) and 8(b), respectively. It is noteworthy that the 'n' value for both viscous solutions is less than 1 ($n < 1$) validating the typical pseudoplastic behaviour of the polymeric solutions. These results are also corroborated with the mechanical properties of the membranes. It is noteworthy that the addition of SWA into the NaAlg-PVA blend increases its mechanical strength and elongation-at-break is decreased. To our knowledge, this is the first study on the rheological behaviour of the precursor solution of any proton-exchange membrane for understanding the processing conditions.

DMFC performance and methanol permeability studies

Fig. 9 (a) and (b) show the DMFC performance curves for MEAs comprising Nafion-117, NaAlg-PVA blend membrane and NaAlg-PVA-HPA mixed-matrix membranes, respectively, at 343 K under atmospheric pressure. The peak power-density for NaAlg-PVA blend membrane is ~30 mW cm^{-2} at a load current-density of ~125 mA cm^{-2}. The peak power-density increased on the addition of HPA to NaAlg-PVA matrices. Hydrated phases of HPA enhance the ionic conductivity as is evident from the improved *I–V* characteristics of mixed matrices shown in Fig. 9(a). Proton-conducting channels offered by the NaAlg-PVA-HPA mixed matrices improve DMFC performance. On comparing the different HPAs, NaAlg-PVA-SWA shows better DMFC performance than the mixed matrices of NaAlg-PVA-PWA and NaAlg-PVA-PMoA. The peak power-density of 68 mW cm^{-2} at load current-density of 225 mA cm^{-2} is observed for NaAlg-PVA-SWA mixed matrices in relation to peak power-density values of 58 and 55 mW cm^{-2} at load current-density values of 200 and 180 mA cm^{-2} observed for mixed matrices of NaAlg-PVA-PWA and NaAlg-PVA-PMoA, respectively. It is noteworthy that SWA with a bigger number of protons in its

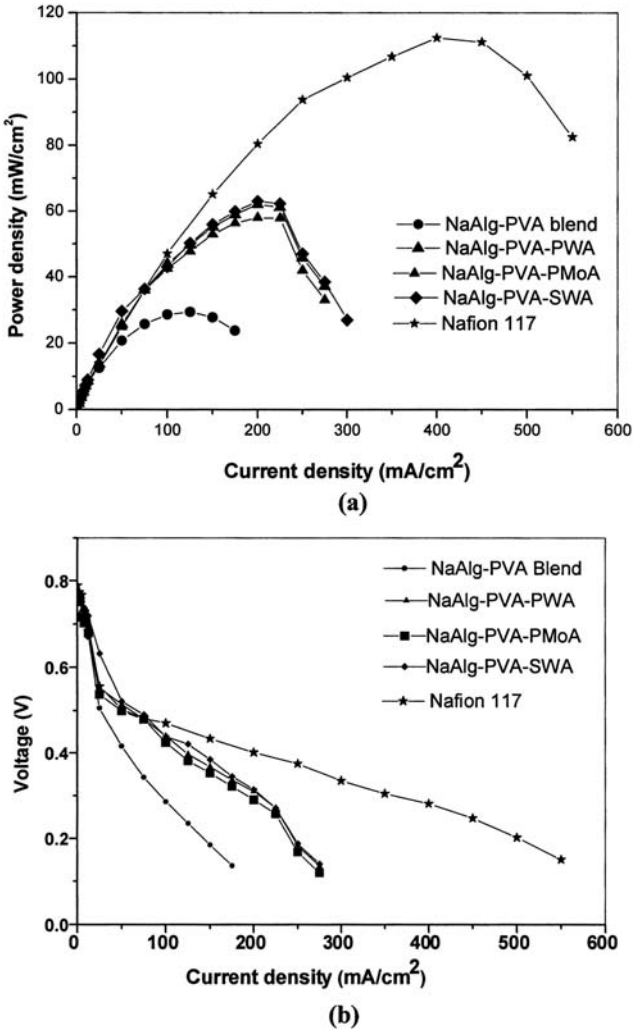

Fig. 9 (a) Cell voltage and (b) power density *vs.* current density for Nafion-117, NaAlg-PVA blend and NaAlg-PVA-HPA mixed matrix membranes.

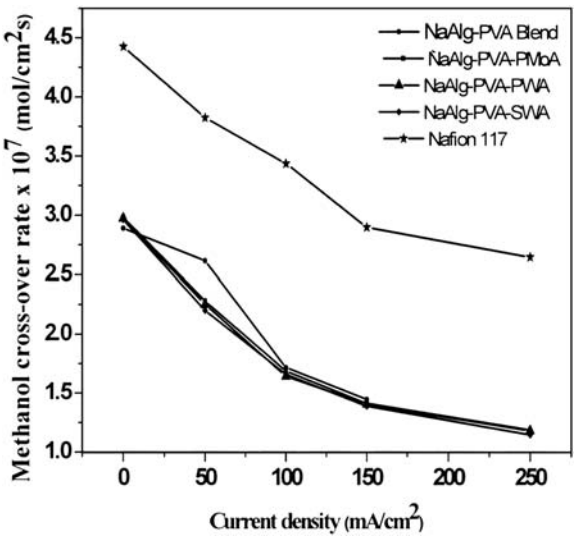

Fig. 10 Methanol-cross-over rate *vs.* current density for Nafion-117, NaAlg-PVA blend, NaAlg-PVA-PWA, NaAlg-PVA-SWA and NaAlg-PVA-PMoA mixed-matrix membranes.

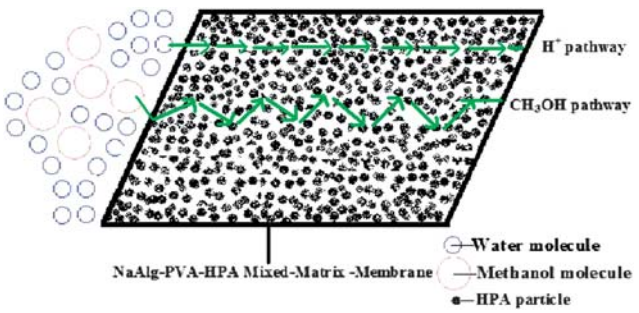

Scheme 3 Restricted methanol and facile proton-pathway through NaAlg-PVA-HPA mixed-matrix membrane

structure offers additional proton conducting sites than PWA and PMoA. However, a peak power-density of 110 mW cm^{-2} at a load current-density of 400 mA cm^{-2} is observed for Nafion-117 membrane which is higher than the mixed matrix-membranes. These results are also in agreement with the proton conductivity data.

Fig. 10 shows the methanol permeability data for Nafion-117 and NaAlg-PVA and NaAlg-PVA-HPA mixed-matrix membranes. It is obvious that methanol permeation decreases with increasing load current-density with a similar trend seen for all the membranes studied here. The methanol cross-over rates for NaAlg-PVA blend membrane and NaAlg-PVA-HPA mixed-matrix membranes are lower in relation to Nafion-117 membrane both under OCV and at varying load current-densities. This is attributed to the higher hydrophilicity of NaAlg-PVA blend and NaAlg-PVA-HPA mixed-matrix membranes that favours the selective sorption of water from the methanol–water mixture. The preferential water-sorption is related to the pervaporation mechanism observed for most of the aqueous–organic mixtures through NaAlg-PVA blend membranes.[16] It is noteworthy that average methanol cross-over rate is lower for NaAlg-PVA blend membrane and NaAlg-PVA-HPA mixed-matrix membranes than Nafion-117 membrane suggesting higher affinity of the NaAlg-PVA polymeric matrix towards water than methanol, which is favourable for the prolonged operation of DMFCs. The methanol cross-over rate differs with the nature of HPAs. NaAlg-PVA-SWA mixed-matrix membrane has a lesser methanol cross-over rate compared to both PWA and PMoA containing mixed matrices. The methanol cross-over rate through the NaAlg-PVA blend membrane is slightly lower in relation to NaAlg-PVA-HPA mixed matrices. By contrast, HPAs in the NaAlg-PVA blend interacts with both water and methanol molecules but due to lower polarity and larger size of methanol molecule in relation to water, the extent of interaction of HPA with methanol molecule is less than water; this helps restricting methanol permeability through the mixed-matrix membrane in DMFCs. This can also be visualized from the Scheme 3.

PVA is primarily responsible for the decrease of methanol cross-over in the membrane. NaAlg-PVA membranes break the water–methanol azeotrope, restricting the methanol cross-over. For a potential DMFC electrolyte, the membrane should possess both proton conductivity and methanol-barrier property.

This journal is © The Royal Society of Chemistry 2010

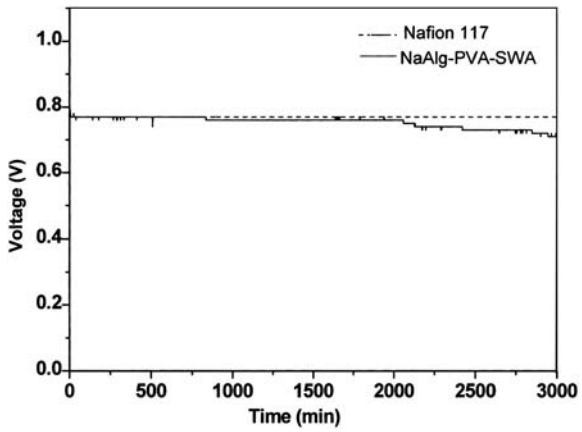

Fig. 11 Durability data depicting the variation in open-circuit voltage with time for Nafion-117 and NaAlg-PVA-SWA mixed-matrix membranes.

Electrochemical selectivity (σ/P) is the ratio of proton conductivity (σ) and methanol permeability (P), which is often used to evaluate the membrane-electrolyte performance in a DMFC. Electrochemical selectivity for NaAlg-PVA blend membrane and NaAlg-PVA-HPA mixed matrices are given in Table 1. NaAlg-PVA blend membrane has lower methanol permeability and lower proton conductivity, and hence its electro-chemical selectivity is lower than NaAlg-PVA-HPA mixed matrix while Nafion membrane has higher ionic conductivity and methanol permeability. However, the electrochemical selectivity of Nafion is higher than NaAlg-PVA-HPA. The ratio of proton conductivity and methanol permeability should be balanced in order to improve the electrochemical selectivity of the membrane in DMFCs. However, in the present membrane, the proton conductivity can be improved by increasing the content of HPAs. Furthermore, methanol permeability is also increased by higher addition of HPAs affecting the overall electrochemical selectivity. Accordingly, reducing the methanol permeability without affecting the proton conductivity of these mixed-matrix membranes is a challenging task and further studies are desired to address these issues. As shown in Fig. 11, the durability of mixed-matrix membrane is verified by monitoring the open-circuit voltage (OCV) for prolonged durations; it is found that NaAlg-PVA-SWA is durable up to 2000 min.

Conclusions

The performance evaluation of NaAlg-PVA-HPA mixed-matrix membranes in DMFCs with selective water-sorption characteristics and methanol-barrier properties is reported for the first time in the literature. Reduced methanol cross-over across NaAlg-PVA and NaAlg-PVA-HPA mixed-matrix membranes in DMFCs is demonstrated. Although NaAlg-PVA-HPA mixed-matrix membranes are cost-effective membrane electrolytes for DMFCs, it is desirable to further their proton conductivity to increase their electrochemical selectivity for enhancing their performance in DMFCs.

Acknowledgements

Financial support under the Supra-Institutional Project from CSIR, New Delhi is gratefully acknowledged.

References

1 E. Antolini, J. R. C. Salgado and E. R. Gonzalez, *Appl. Catal., B*, 2006, **63**, 137–149.
2 N. W. Deluca and Y. A. Elabd, *J. Polym. Sci., Part B: Polym. Phys.*, 2006, **44**, 2201–2225.
3 V. Neburchilov, J. Martin, H. Wang and J. Zhang, *J. Power Sources*, 2007, **169**, 221–238.
4 P. D. Beatie, F. P. Orfino, V. I. Basura, K. Zychowska, J. Ding, C. Chuy, J. Scmeisser and S. Holdcroft, *J. Electroanal. Chem.*, 2001, **503**, 45–56.
5 M. L. Ponce, L. A. S. de, A. Prado, V. Silva and S. P. Nunes, *Desalination*, 2004, **162**, 383–391.
6 V. S. Silva, S. Weisshaar, R. Reissner, B. Ruffmann, S. Vetter, A. Mendes, L. M. Madeira and S. Nunes, *J. Power Sources*, 2005, **145**, 485–494.
7 A. K. Sahu, S. D. Bhat, S. Pitchumani, P. Sridhar, V. Vimalan, C. George, N. Chandrakumar and A. K. Shukla, *J. Membr. Sci.*, 2009, **345**, 305–314.
8 B. Smitha, S. Sridhar and A. A. Khan, *Macromolecules*, 2004, **37**, 2233–2239.
9 L. Li, L. Xu and Y. Wang, *Mater. Lett.*, 2003, **57**, 1406–1410.
10 D. S. Kim, H. B. Park, J. W. Rhim and Y. M. Lee, *J. Membr. Sci.*, 2004, **240**, 37–48.
11 C. W. Lin, Y. F. Huang and A. M. Kannan, *J. Power Sources*, 2007, **171**, 340–347.
12 A. K. Sahu, G. Selvarani, S. Pitchumani, P. Sridhar, A. K. Shukla, N. Narayan, A. Banarjee and N. Chandrakumar, *J. Electrochem. Soc.*, 2008, **155**, B686–695.
13 S. D. Bhat, A. K. Sahu, C. George, S. Pitchumani, P. Sridhar, N. Chandrakumar, K. K. Singh, N. Krishna and A. K. Shukla, *J. Membr. Sci.*, 2009, **340**, 73–83.
14 S. Mohanapriya, S. D. Bhat, A. K. Sahu, S. Pitchumani, P. Sridhar and A. K. Shukla, *Energy Environ. Sci.*, 2009, **2**, 1210–1216.
15 M. Yamada and I. Honma, *Electrochim. Acta*, 2005, **50**, 2837–2841.
16 S. D. Bhat and T. M. Aminabhavi, *J. Membr. Sci.*, 2007, **306**, 173–185.
17 U. S. Toti and T. M. Aminabhavi, *J. Membr. Sci.*, 2004, **228**, 199–208.
18 S. D. Bhat and T. M. Aminabhavi, *Sep. Purif. Rev.*, 2007, **36**, 203–229.
19 C. K. Yeom and K. H. Lee, *J. Appl. Polym. Sci.*, 1998, **67**, 949–959.
20 S. G. Adoor, B. Prathab, L. S. Manjeshwar and T. M. Aminabhavi, *Polymer*, 2007, **48**, 5417–5430.
21 M. D. Kurkuri, J. N. Nayak, M. I. Aralaguppi, B. V. K. Naidu and T. M. Aminabhavi, *J. Appl. Polym. Sci.*, 2005, **98**, 178–188.
22 A. Heydari, S. Khaksar, M. Sheykhan and M. Tajbakhsh, *J. Mol. Catal. A: Chem.*, 2008, **287**, 5–8.
23 I. Colicchio, F. Wen, H. Keul, U. Simon and M. Moeller, *J. Membr. Sci.*, 2009, **326**, 45–57.
24 M. J. Janik, R. J. Davis and M. Nerco, *J. Phys. Chem. B*, 2004, **108**, 12292–30.
25 O. Nakemura, T. Kodama, I. Ogino and Y. Miyake, *Chem. Lett.*, 1979, 17–18.
26 J. Sauk, J. Byun and H. Kim, *J. Power Sources*, 2005, **143**, 136–141.
27 T. Uma and M. Nogami, *J. Electrochem. Soc.*, 2007, **154**, B845.
28 A. A. Juan, B. Salvador and G. Pedor, *Electrochem. Commun.*, 2003, **5**, 967–972.
29 G. Pedor, A. A. Juan and B. Salvador, *Electrochim. Acta*, 2005, **50**, 4715–4720.
30 M. Yamada and I. Honma, *J. Phys. Chem. B*, 2006, **110**, 20486–20490.
31 M. Aparicio, Y. Castro and A. Duran, *Solid State Ionics*, 2005, **176**, 333–340.
32 U. L. Stangar, N. Groselj, B. Orel and P. Colomban, *Chem. Mater.*, 2000, **12**, 3745–3753.
33 M. Aparicio, J. Mosa, M. Etienne and A. Durán, *J. Power Sources*, 2005, **145**, 231–236.
34 V. Ramani, H. R. Kunz and J. M. Fenton, *Electrochim. Acta*, 2005, **50**, 1181–1187.
35 V. Ramani, H. R. Kunz and J. M. Fenton, *Electrochim. Acta*, 2005, **50**, 1181–1187.
36 S. Soled, G. Misceo, Mc Vicker, W. E. Gates, A. Guiterrez and J. Paes, *Catal. Today*, 1997, **36**, 441–450.
37 S. Kang, S. J. Lee and H. Chang, *J. Electrochem. Soc.*, 2007, **154**, B1179–B1185.
38 Y. C. Chen, C. S. Jer, L. K. Tong, C. W. Chen, L. C. Tseng and H. C. An, *J. Power Sources*, 2008, **184**, 44–51.

39 K. Y. Song, H. K. Lee and H. T. Kim, *Electrochim. Acta*, 2007, **53**, 637–643.
40 R. H. Perry, D. W. Green, J. D. Maloney in *Perry's Chemical Engineers Hand Book*, 7th edition, McGraw-Hill, 1997.
41 R. Jiang and D. Chu, *J. Electrochem. Soc.*, 2004, **151**, A69–A76.
42 A. Anis, A. K. Banthia and S. Bandyopadhyay, *Journal of Materials Engineering and Performance*, 2008, **17**, 772–779.
43 C. Schmidt, T. Gluck and G. S. Naake, *Chem. Eng. Technol.*, 2008, **31**, 13–22.
44 J. Crank, *The Mathematics of Diffusion*, 1975, Clarendon Press, Oxford, UK.
45 K. D. Kreuer, *Solid State Ionics*, 2000, **136–137**, 149–160.
46 K. D. Kreuer, *Chem. Mater.*, 1996, **8**, 610–641.
47 K. D. Kreuer, *J. Membr. Sci.*, 2001, **185**, 29–39.
48 A. Horky, N. P. Kherani and G. Xu, *J. Electrochem. Soc.*, 2003, **150**, A1219–1224.
49 B. B. Bardin, S. V. Bordawekar, M. Nerco and R. J. Davis, *J. Phys. Chem. B*, 1998, **102**, 10817–10825.
50 T. Kukino, R. Kikuchi, T. Takeguchi, T. Matsui and K. Eguchi, *Solid State Ionics*, 2005, **176**, 1845–1848.
51 M. Langpape, J. M. M. Millet, U. S. Ozkan and M. Boudeulle, *J. Catal.*, 1999, **181**, 80–90.
52 B. Smitha, S. Sridhar and A. A. Khan, *J. Appl. Polym. Sci.*, 2005, **95**, 1154–1163.
53 Z. Cui, W. Xing, C. Liu, J. Liao and H. Zhang, *J. Power Sources*, 2009, **188**, 24–29.
54 M. D. Leal, B. Matsuhiro Rossi and F. Caruso, *Carbohydr. Res.*, 2008, **343**, 308–316.
55 M. Mancini, M. Moresi and F. Sappino, *J. Food Eng.*, 1996, **28**, 283–295.
56 P. Prentice, Rheology and its role in plastic processing, *Science*, 1995, **Vol. 1**(Ch. 1), 1–11.

 This journal is © The Royal Society of Chemistry 2010